HHS Public Access

Author manuscript

Neuroimage. Author manuscript; available in PMC 2018 July 01.

Published in final edited form as:

Neuroimage. 2017 July 01; 154: 33–42. doi:10.1016/j.neuroimage.2016.11.014.

Prospective Motion Correction in Functional MRI

Maxim Zaitsev, Ph.D[*], **Burak Akin**, **Pierre LeVan, Ph.D**, and **Benjamin R. Knowles, Ph.D**

Department of Radiology – Medical Physics, University of Freiburg – Medical Centre, Freiburg, Germany

Abstract

Due to the intrinsic low sensitivity of BOLD-fMRI long scanning is required. Subject motion during fMRI scans reduces statistical significance of the activation maps and increases the prevalence of false activations. Motion correction is therefore an essential tool for a successful fMRI data analysis. Retrospective motion correction techniques are now commonplace and are incorporated into a wide range of fMRI analysis toolboxes. These techniques are advantageous due to robustness, sequence independence and have minimal impact on the fMRI study setup. Retrospective techniques however, do not provide an accurate intra-volume correction, nor can these techniques correct for the spin-history effects. The application of prospective motion correction in fMRI appears to be effective in reducing false positives and increasing sensitivity when compared to retrospective techniques, particularly in the cases of substantial motion. Especially advantageous in this regard is the combination of prospective motion correction with dynamic distortion correction. Nevertheless, none of the recent methods are able to recover activations in presence of motion that are comparable to no-motion conditions, which motivates further research in the area of adaptive dynamic imaging.

Keywords

function MRI; fMRI; motion correction; prospective motion correction; real-time motion correction; adaptive dynamic MRI

Magnetic resonance imaging (MRI) is an indispensable tool for studying brain morphology and function. Although MRI provides great diagnostic and prognostic value, it is also notorious for a host of artefacts, which often affect the quality of the acquired data and reliability of the conclusions. Motion artefacts in traditional MR imaging have an extremely volatile appearance, but typically they can be represented as a combination of blurring and ghosting (Lauzon and Rutt, 1993; Van de Walle et al., 1997; Wood and Henkelman, 1985). The exact manifestation of motion artefacts is related to the way in which inconsistent raw data acquired in different motion states are combined into a single k-space dataset prior to

[*]Corresponding author: Maxim Zaitsev, Department of Radiology - Medical Physics, University Medical Centre Freiburg, Breisacher Str. 60a, 79106, Freiburg, Germany. Phone: +49 761 27074120, Fax: +49 761 27093790, zaitsev@ukl.uni-freiburg.de.

There are no financial interests or commercial products associated with the presented material.

the Fourier transform. These artefacts arise mainly due to the prolonged period of time required to form a complete k-space dataset. For more detail on artefacts in traditional MRI interested reader is referred to recent reviews on the topic (Godenschweger et al., 2016; Zaitsev et al., 2015). In contrast, functional MRI (fMRI) is typically carried out using 2D single-shot signal readouts (Tsao, 2010). Such readout modules are in most cases under 100ms in duration and are hence said to “freeze” motion, with regards to the majority of physiological motion types. Therefore individual 2D images resulting from single-shot acquisitions are indeed free of the “classical” MRI motion artefacts. Nonetheless, in the case of fMRI, volumetric data are required, which are produced by the sequential acquisition of multiple 2D slices, with characteristic acquisition times in the range of one to several seconds. Even though recent approaches such as simultaneous multi-slice (SMS) allow for shortening of these times by a significant factor (Barth et al., 2016), fast physiological motion may still produce volume distortions and cause crosstalk between different slices, resulting in intra-volume data inconsistencies. More importantly, fMRI acquisitions consist of repetitive scanning of the same volume, in which the temporal evolution of the signal in every voxel serves as a basis for the statistical analysis (Cox, 1996; Friston et al., 1995; Goebel et al., 2006). Motion in this case results in inconsistencies between the subsequently acquired image volumes across the time series, giving rise to inter-volume data instabilities. Although these may not lead to apparent artefacts in the images, they may substantially deteriorate the statistical analysis and distort the results.

Influence of motion on fMRI data

Subject motion during fMRI acquisitions is considered to be one of the major confounding factors affecting data quality (Haller and Bartsch, 2009; Van Dijk et al., 2012). According to recent assessments, involuntary subject motion in typical fMRI experiments in young motivated volunteers is approximately in the range of 1 to 2 mm and rotations of approximately 1° are not uncommon. In the case of patients, elderly and children however, substantially more obtrusive motion is oft observed (Mayer et al., 2007; Seto et al., 2001; Yuan et al., 2009). Most prominent types of motion include nodding (head rotations around the left-right axis of the subject) combined with translations along the anterior-posterior and inferior-superior directions, and translations along the inferior-superior direction associated with limb motion and body posture changes. Such head motions result in local displacements of the anatomic brain features to a significant fraction of the voxel size, leading to a variety of physical phenomena, all contributing to an undesired temporal variation of the voxel signal evolution. The most substantial of these factors are listed in Table 1.

In the case of head imaging 3T or below, the transmit field can be considered homogeneous and both transmit and receive coil sensitivities independent of head position for the range of the relevant subject motion. However at higher field strengths, such as 7T or 9.4T, points 1, 2 and 5 may increase in importance (Faraji-Dana et al., 2016; Tian et al., 2015). Point 3 is directly relevant for fMRI as it leads to the well-known spin-history effects (Yancey et al., 2011), most prominently observed in fast functional protocols with TR times on the order of the typical longitudinal relaxation times of the relevant brain tissues. Motion of the anatomic structures with respect to the encoding coordinates (point 6) leads to dramatic effects if left

uncorrected, resulting in signal variations significantly exceeding the expected BOLD signal variations. Fortunately, there are a wide range of retrospective motion correction algorithms to rather effectively address this problem (Friston et al., 1995; Jenkinson et al., 2002). Gradient non-linearity correction (point 8) may also be integrated into the reconstruction and analysis pipeline (Yarach et al., 2015), however, for the typical range of motions and relatively low spatial resolution characteristic for the majority of fMRI studies, these effects are mostly negligible. Motion of anatomical structures relative to the generally very inhomogeneous receiver coil sensitivities of the typical receiver arrays produces a position-variant weighting of the corresponding signals. This can be undone by an appropriate channel combination method (Pruessmann et al., 1999; Roemer et al., 1990), which however rely on knowledge of the coil sensitivity profiles, which may change in presence of substantial movements. This is especially critical for protocols employing parallel imaging (Griswold et al., 2002; Pruessmann et al., 1999) or simultaneous multi-slice acceleration (Feinberg and Setsompop, 2013), as motion in this case may result in position-dependent g-factor penalty variations or oscillating levels or residual aliasing.

As seen from the list in Table 1, a substantial number of effects related to motion are associated with the magnetic field homogeneity alterations. Although the homogeneity of the main magnetic field may in some cases be limited by technical constraints, typically the most significant source of the magnetic field distortion is the presence of the subject inside the bore of the magnet. Variations in the magnetic field susceptibility between the air and the tissues, as well as amongst the different tissue types, in combination with the complex shape of the body and internal anatomical structures, result in substantial deviations of the local resonant frequencies within the object of investigation. For example, in head imaging the magnetic field distribution within the brain results from a superposition of the field from the head directly, but also substantial contributions from the shoulders, chest, lungs and upper limbs. A static shimming procedure is typically performed prior to the functional scan, which attempts to counteract the overall magnetic field inhomogeneity in the target region without differentiating the sources of the corresponding contributions. Motion of the head relative to the rest of the body and the shimming coils results in the manifestation of complex magnetic field inhomogeneities (Ooi et al., 2013b; Yarach et al., 2016). Furthermore, rotation of the head about any axis non-parallel to the main magnetic field direction causes the field deviations arising from head tissues to change; they do not simply move in synchrony with the head (Maclaren et al., 2013; Ooi et al., 2013b), as can be seen in Figure 1. Although global (e.g. averaged over the object or slice) B0 changes are dynamically measured and compensated for on the majority of the clinical imaging platforms by adjusting the system’s reference frequency or applying appropriate phase corrections, localised changes in the magnetic field distributions are left uncorrected at present.

Magnetic field inhomogeneities are well known to produce geometric distortions as well as signal pile-up and signal void artefacts in images from MR pulse sequences with extended readouts (Jezzard, 2012; Tsao, 2010). Another relevant but less well known effect of the inhomogeneous fields is that the local susceptibility-induced gradients may also affect image contrast and therefore the effective BOLD sensitivity (Deichmann et al., 2002). Dynamic alterations of the magnetic field inhomogeneity add an undesired time variance to geometric

distortions and therefore to the BOLD signal. Attempts to compensate for a whole host of the dynamic field homogeneity effects have been made (Lu et al., 2015), but a broader validation of such laborious approaches is yet to be performed.

It is reasonable to relate the motion occurring in the fMRI experiment and its effects on the data to the voxel size of the underlying imaging method. Signals from larger voxels are less affected by the direct geometric effects associated with certain anatomic structures entering or leaving the voxel upon motion. This is mainly due to the signal averaging over a larger volume. At the same time low-resolution EPI (as well as other single-shot techniques) has a shorter readout time and hence a reduced sensitivity to motion-induced B0 alternations. Hence, although there is no strict mathematical formalism available for fMRI time series similar to that of Maclaren et al. (Maclaren et al., 2010) for conventional imaging, a ratio of a typical displacement within the brain region to the voxel dimensions is a good measure of the severity of motion. Another measure of motion severity is its speed, which can be translated into displacements using characteristic times in the acquisition protocol, e.g. k-space readout duration, or TR. The former is relevant to assess k-space deteriorations (typically irrelevant for fMRI), while the latter relates to the intra-volume distortions (point 7 in Table 1).

As can be seen, there are many possible mechanisms for data corruption resulting from subject motion and correspondingly many different strategies may be required to address these challenges. The most obvious and effective method of suppressing all motion-related artefacts is to preemptively prevent or limit motion. If motion can be avoided, then the effects discussed above are avoided and other, more complex, strategies become redundant. Unfortunately, preventing motion is not always practical, especially in fMRI settings. For instance, clinical imaging of infants can be timed after feeding to take advantage of sleeping (Windram et al., 2012), whereas in young children, sedation can be employed (Malviya et al., 2000). Functional MRI, however, typically requires the subject to be awake. In the early days of MRI, bite bars mounted on head coils (Bettinardi et al., 1991; Menon et al., 1997) were deemed effective in avoiding head motion. However, due to their cumbersome set up and significant discomfort, immobilizing systems have not found wide acceptance. Training with a mock MRI setups appears to be useful to avoid bulk motion by reducing anxiety, both in children and patients (de Bie et al., 2010; Lueken et al., 2012; Malisza et al., 2012). Also feeding back subject motion in real-time, as detected from MR data or using additional devices (Yang et al., 2005), appears to be effective and was reported to only minimally interfere with the main task.

Retrospective motion correction approaches and their imitations

Retrospective image realignment is currently the method of choice for the majority of fMRI studies. A number of algorithms are available, as included in commonly used fMRI analysis packages such as SPM, FSL, AFNI or BrainVoyager (Cox, 1996; Friston et al., 1995; Goebel et al., 2006; Jenkinson et al., 2002). Although there are differences in the details of the approaches used in these packages, as well as variations in the recovered motion trajectories, all appear to produce similar results in terms of the detected activations (Oakes et al., 2005). Most of the retrospective motion correction algorithms use a rigid body motion

model, assuming the entire volume transformation can be described by 6 parameters: three rotations and three translations, known as six degrees of freedom (6DoF) motion. Typically, these algorithms operate on successive image volumes assuming an idealized voxel function and relying on interpolation in the image domain to undo the effect of the detected motion. They also implicitly assume that motion only occurs once per volume acquisition, ignoring a potential misalignment between the individual slices within each volume. Differences between the various realignment options lie in the details of the interpolation algorithms and cost functions used and the optimization approaches to minimize (or maximize) the respective cost function.

Uncorrected or insufficiently corrected motion introduces strong dynamic modulations into the fMRI data, especially close to the high-contrast borders. If motion does not correlate with the task, then these modulations are treated by the analysis software as noise, leading to a decrease in significance and reduction of the detected activations. In addition, even a weak correlation to the task results in the appearance of false activations (Hajnal et al., 1994). In resting-state fMRI, uncorrected motion effects tend to decrease detected functional coupling across the distributed networks, while apparently increasing the local functional coupling (Van Dijk et al., 2012).

It is common to account for residual inaccuracies in motion-corrected data by including the detected motion traces into the fMRI data analysis. For task-based fMRI, motion parameters detected in the realignment step are often included as additional regressors in the general linear model (GLM) analysis (Friston et al., 1996; Hutton et al., 2011). This assumes simple relations (e.g. linear or quadratic) of the residual motion-induced signal variations with regard to detected displacements or motion velocity, and appears to systematically reduce the signal variance (Lund et al., 2005). Nonetheless, some studies report that low amplitude movements weakly-correlated to the stimulus may still result in false activations (Field et al., 2000). In resting-state fMRI, the microscopic sub-voxel movements are a source of large concern (Murphy et al., 2013), introducing potential bias in group analysis if the different groups are characterised by varying likelihoods of motion. Even after regressing out motion-relevant parameters, data censoring, commonly referred to as “scrubbing” is often necessary (Carp, 2013; Power et al., 2014). Despite these efforts, a recent comprehensive study comparing different correction approaches concluded that none of the tested techniques were able to effectively remove motion-induced brain networks differences (Yan et al., 2013).

One of the reasons why the aforementioned data corrections may still be required is that the common image realignment methods ignore the changes in geometric image properties associated with motion. Ignoring B0-induced image distortions by performing rigid-body image realignment prior to the distortion correction results in both incorrect motion estimates and limits the ability of the realignment procedure to eliminate motion-induced signal variance (Wu et al., 1997). A number of dynamic distortion-correction approaches have been proposed recently, e.g. (Dymerska et al., 2015; Lamberton et al., 2007; Yeo et al., 2008). Some of the proposed approaches demand motion estimates for the realignment of the previously acquired initial distortion map and rely on the temporal stability of both the transmit and receive RF fields, which may potentially limit the accuracy of corrections. Others require modification of the acquisition sequence, e.g. alternating the echo times or

phase encoding directions, which may interfere with the temporal sampling accuracy due to the additionally introduced signal modulation. Including the image phase into the reconstruction is a viable option (Hutton et al., 2013), but the accuracy of the underlying assumptions still have yet to be verified, in particular at higher magnetic field strengths. The usability of the dynamic distortion correction as a means to disentangle motion-to-distortion interaction and correct the fMRI time series is yet to be confirmed in a wider range of fMRI studies.

Another limitation of the retrospective volume-by-volume image registration is that it commonly ignores the intra-volume effects that occur during the acquisition of the respective multi-slice packages (point 7 in Table 1). As seen in Figure 2, depending on the order of the acquisition, distortions and transient signal modulations may arise, with different visual appearances. In interleaved acquisitions, striping patterns occur, whereas the sequential ordering results in a more benign artefact appearing as a localized stripe. Although the latter seems to be less destructive to the data, the former is easier to detect as an artefact. Muresan et al. (Muresan et al., 2005) have proposed an algorithm for detecting image voxels affected by spin-history effects based on the different temporal footprints of the tissues with varying T1 relaxation times, which however did not seem to find a wide acceptance in in vivo fMRI studies. Some algorithms account for intra-volume motion (Beall and Lowe, 2014; Bhagalia and Kim, 2008) by performing slice-to-volume registration and using these high-temporal resolution motion traces as nuisance regressors in GLM analysis. Spatio-temporal modelling of the detected functional responses also appears to be of benefit if the paradigm is known to induce motion and precise timing data are available (Lemmin et al., 2010). Ultimately, adaptive correction of slice positions using external high-temporal resolution motion data (Yancey et al., 2011) appears to be a truly viable approach, which is one of the motivations for the methods presented below.

Prospective motion correction approaches

Prospective motion correction relies on the simple and intuitive principle of maintaining a constant relationship between the object under investigation and the imaging slice or volume. It is intuitively apparent that such prospective (a.k.a. adaptive or real-time) motion correction should be possible for the motion of any rigid body, such as the head to a good approximation, in the same way a technologist may re-position slices in a repeated session by locating anatomical landmarks. From a mathematical analysis of the Bloch equations and imaging principles, it follows that any affine motion (of which 6DoF rigid body motion is a subset) may be accounted for equivalently both in image space as well as during the acquisition (Atkinson and Hill, 2003; Maclaren et al., 2013; Nehrke and Börnert, 2005; Zahneisen and Ernst, 2016). From these publications it follows that an arbitrary rigid body motion can be compensated for perfectly if accurate and time-synchronized rotations are applied to the gradients in combination with modifications of transmit and receive phases and frequencies. It is instructive for the analysis of the prospective motion correction approaches to separate the process of collecting the motion information (i.e. navigation or tracking) from the application of the corresponding corrections. In the example above the technologist collects the motion information based on the position of certain landmarks in the images and applies the correction by moving and rotating the slice package, which is

transformed to gradient rotation matrices, frequency and phase settings by the scanner software.

To the best of our knowledge, the earliest use of the term “prospective motion correction” in MRI dates back to 1996 (Lee et al., 1996) where navigator-based motion correction was applied to fMRI, initially for simple translations and two years later for rotations as well (Lee et al., 1998). Correction of all six degrees of freedom was first mentioned by Eviatar et al. in 1997 (Eviatar et al., 1997) in an ISMRM abstract. Two years later the same group presented a first truly real-time prospectively-corrected echo-planar imaging method with a target application in fMRI and a latency of approximately 6 ms and a claimed spatial resolution of 100 μm (Eviatar et al., 1999). The authors used three solid-state laser-based position sensitive detectors mounted outside the magnet and three glass reflectors mounted on the head of the subject to track head motion independently of the MR system. Unfortunately, neither of these two studies seem to have been published as full papers, nor were they followed upon. Around the same time a paper of Derbyshire et al. appeared demonstrating 6DoF motion correction for structural MRI using fiducial markers with integrated RF micro-coils (Derbyshire et al., 1998). Image-based motion detection was also recognised as a viable possibility primarily due to the increased computing power available in the scanner controller, leading to a successful implementation of the prospective acquisition correction (PACE) framework (Thesen et al., 2000) for functional MRI. In PACE, each 3D volume was registered to the reference image directly at the scanner once the data became available and fed back to the sequence control unit to update scanning parameters. Image reconstruction and registration required several hundred milliseconds, which could either be introduced as an inter-volume delay, or used to correct the second next volume acquisition if a delay-free fMRI protocol was desired. A first successful implementation of real-time 6DoF motion correction based on external optical tracking for a range of MR pulse sequences, including EPI was published as a paper in 2006 (Zaitsev et al., 2006). In this work, a slightly modified commercial optical tracking system was used, positioned outside of the scanner bore and monitoring a set of retro-reflective spheres attached to the subject using a dental impression. This work had been preceded in a number of ISMRM abstracts in 2004 to 2006 from the same group using prototype tracking systems and less efficient sequence implementations, most notably demonstrating slice-by-slice correction for EPI (Zaitsev et al., 2004) and initial fMRI results (Speck and Zaitsev, 2006).

Prospective motion correction is a very generic and powerful approach. For fMRI applications it is the only technique that allows for an adequate correction of spin-history effects (Yancey et al., 2011) and intra-volume distortions (Speck et al., 2006). Furthermore, it simplifies the motion-to-distortion interaction by aligning the phase-encoding direction with the underlying anatomy. Upon arbitrary head motions, some components of the local inhomogeneities can be considered to move together with the head, whereas the other components remain stationary or experience more complex changes. If the latter component is negligible, prospective motion correction would achieve a perfect correction of both motion and dynamic changes in geometric distortions. In a more realistic scenario, dynamic distortions in prospectively corrected images will still be present; however, the problem of correcting these reduces from two dimensions to one- (see Figure 3). Due to this simplification, distortion correction in prospectively motion-corrected echo-planar images is

greatly simplified, provided dynamic distortion information is available. In case of phantom imaging, such information may be derived from a known structure of the object and a forward calculation of the susceptibility-induced field distortion (Boegle et al., 2010). In our group we evaluated an option of creating a susceptibility model of the head based on MR data (Sostheim et al., 2012), which initially showed promise but failed to achieve the desired accuracy of field prediction. Other approaches based on direct estimation of the B0 field changes have been presented recently (Ooi et al., 2013b; Rotenberg et al., 2013), which demonstrate the efficacy of distortion correction following prospective motion correction.

Common pitfalls associated with prospective motion correction

Along with the power of prospective motion correction come a number of caveats. As true for any feedback chain introduced to a complex system, prospective motion correction may potentially destabilise the imaging results through measurement noise, instabilities, calibration errors, marker drifts or malfunction. One of the more irksome practical problems is that no “uncorrected” images can be extracted from an experiment if data were acquired with prospective correction. Although an approximation of undoing the effects of prospective correction has been recently proposed (Zahneisen et al., 2016) it can only be used for demonstration purposes and is not relevant to typical fMRI protocols. Therefore, a major constraint exists in performing validation studies, as separate runs are required for scans with and without prospective motion correction, whereas the conditions involving involuntarily motions are not reproducible by definition.

Accuracy and precision requirements for spin-warp MRI have been analysed recently (Maclaren et al., 2010; Zahneisen et al., 2014a), however, no similar studies are known to the authors that focus on fMRI-specific aspects. For traditional imaging, the tracking data precision must be greater than a fraction of the voxel size and is related to the contrast of the image. A general rule of thumb that $1/5^{th}$ to $1/10^{th}$ of the target voxel size is sufficient for the majority of applications (Maclaren et al., 2010; Stucht et al., 2015). Although as the typical fMRI voxel size is much larger than that of structural imaging, one can expect that more stringent specifications may apply.

The motion detection process is always associated with a certain latency, defined as the duration between the movement of the imaging object and the first scanning event which readily accounts for this motion. For navigator-based methods, time is required to play out the gradients and RF pulses as well as to record the data and to reconstruct the motion parameters. For camera-based tracking, optical images are typically taken frame-by-frame, followed by the transfer to an external computer and subsequent calculations. The latter may include complicated computer vision algorithms which further contribute to the tracking delay. Also included in the latency is the transfer of the 6DoF data to the scanner controller, and incorporation of the updates into the running sequence. It is therefore important to measure and characterise system latency, e.g. by measuring a residual displacement in presence of continuous motion (Zaitsev et al., 2006). Latency requirements in fMRI may generally be rather stringent, but will be highly dependent of the types of motion expected. For example, an appropriate correction of cardio-ballistic bulk head motion requires a latency below 20 ms (Herbst et al., 2014).

In a correctly implemented prospectively-corrected MR experiment, the imaged object, e.g. the head, remains stationary in the logical slice coordinate system upon any arbitrary subject motion. Consequently, stationary objects, such as RF, gradient and shim coils appear now to move in the direction opposite to the true object motion. This apparent motion complicates the application of retrospective intensity and gradient non-linearity correction; however it does not change anything regarding the underlying MR physics. Therefore accurate compensation of these effects is feasible upon the application of the appropriate (known at the time of image reconstruction) spatial transformations (Yarach et al., 2016, 2015).

Rotation of the imaging coordinates relative to the gradients introduces an additional potential source of artefact related to the anisotropy of the gradient performance characteristics. Different physical gradient axes are known to have different delays and eddy-current characteristics. For different orientations the k-space errors may have different realisations. Single-shot readouts such as EPI are especially susceptible to these errors due the very high gradient amplitudes and slew rates used. In EPI this typically results in orientation-dependent eddy-current induced distortions and ghosting. As seen from the example in Figure 4, standard vendor-supplied ghost suppression technique fails upon any substantial rotation and alternative advanced ghost suppression techniques may be required, such as PLACE (Rotenberg et al., 2013; Xiang and Ye, 2007), or potentially other approaches (Chen and Wyrwicz, 2004; Hennel, 1999; Vannesjo et al., 2016).

Navigator-based methods (Alhamud et al., 2012; Fu et al., 1995; Gallichan et al., 2016; Thesen et al., 2000; van der Kouwe et al., 2006; Ward et al., 2000; Welch et al., 2002; White et al., 2010) use the MR image data for motion detection. These methods typically have increased latency compared to optical tracking, which decreases the acquisition speed of the main imaging sequence, but has two advantages: the detected motion is directly related to the motion of the object of interest and is represented in the same coordinate frame. Some approaches use additional devices, e.g. MR-visible markers (Ooi et al., 2013a, 2011; Sengupta et al., 2014), where the detected motion is still in MR reference frame, but rigid coupling between the markers and the object is not necessarily present and additional measures need to be taken in order to ensure such coupling. Finally, for truly external motion tracking devices (Forman et al., 2010; Maclaren et al., 2012; Rotenberg et al., 2013; Schulz et al., 2012; Zaitsev et al., 2006), both marker fixation and coordinate frame matching need to be ensured. The latter is typically achieved by a cross-calibration procedure (Zahneisen et al., 2014b; Zaitsev et al., 2006). The former, however, is sometimes easier to realise for optical tracking because the markers can be made as small as 15mm (Maclaren et al., 2012). A compromise between the subject comfort and the security of coupling (Maclaren et al., 2013) remains challenging, with the dental fixation method still being the method of choice if high accuracy is required (Stucht et al., 2015).

Experimental fMRI studies employing prospective motion correction

When comparing the efficacy of different motion correction approaches it is often useful to consider whether the study conclusions are concerned with fast and large-scale motion conditions as opposed to microscopic subconscious, unintended motions, as in these cases various phenomena contribute differently to the resulting signal evolutions. Furthermore, as

there is to date no perfect correction available, and considering motion sampling rate limitations, latency, and accuracy constraints, relative improvements and residual confounds may appear to be very different depending on how prospective motion correction is implemented. In our early test fMRI study (Speck et al., 2006), we considered large scale rotations, on the order of 15° accompanied with translations of several centimetres, performed by the subjects according to instructions provided during the scanning session. Under these conditions external prospective correction clearly outperformed both purely retrospective and PACE correction. However, despite the prospective motion correction, scans in the presence of intended motion have shown reduced activation. A later study based on active marker tracking has shown a consistent positive effect of the prospective motion correction under conditions of smaller but substantial motions, confirming however, the inability of achieving perfect corrections in case of motion and attributing this to motion-induced B0 variations (Ooi et al., 2011). Soon after, the same group presented a method for prospective motion correction combined with dynamic retrospective distortion correction (Ooi et al., 2013b) and applied it successfully to a 12-subject group fMRI study performed under physiological unconscious motion conditions (Muraskin et al., 2013). They have found a small but significant increase in Z-scores brought about by the prospective motion correction, which surprisingly could be attributed to an increase in the effect strength rather than decrease of the signal variance. Another study based on an optical stereoscopic in-bore tracking system and finger-tapping experiment in a relatively small cohort has independently demonstrated the importance of the dynamic distortion correction for reduction of false activations in the case of substantial motion (Rotenberg et al., 2013). In contrast to the study of Muraskin et al, they have shown a reduction of activation in the no-motion + correction condition, which they attributed to the decrease of false positive activations in the motor area. A right leg movement paradigm, known to induce stimulus-correlated motion, was studied in 15 participants in combination with an embedded optical motion tracking device and slice-by-slice motion correction without additional distortion correction (Schulz et al., 2014). In this paper the authors demonstrated a robust and significant reduction in false activations, but at the same time note the necessity of dynamic distortion correction.

In our lab we have recently performed another pilot study involving 2D-EPI fMRI experiments using a block design unilateral right-handed finger-tapping paradigm, with stimuli blocks of 20s duration followed by 20s control. To date, eleven participants were included in the study. The volunteers were instructed to stay as still as possible during the session. An optical motion tracking camera (Metria Innovation Inc., Milwaukee, WI) was used to track the position of a marker attached using two-sided adhesive tape to the nose bridge of the subject. Marker fixation to the skin of the subject was selected to test the hypothesis, that it could provide sufficiently rigid coupling in young motivated volunteers. All scans were performed on a 3T Magnetom Prisma using a 64 channel Tx/Rx head coil (Siemens Healthineers, Erlangen, Germany). MRI protocol consisted of an isotropic MPRAGE, followed by an EPI sequence with parameters: 64×64 matrix size; TE=30ms; $4mm^2$ in-plane resolution; 30 slices of 5mm thickness. In each scan, 180 measurements were acquired with a TR of 2s, leading to a scan duration of 360s (6mins). The EPI scan was repeated 2–3 times with and without prospective motion correction. No retrospective distortion correction was applied. During the offline post-processing, retrospective motion

correction (Jenkinson et al., 2002) was applied to all scans, forming image datasets with: no motion correction; prospective only; retrospective only; and with both prospective and retrospective correction. Data were analysed in terms of temporal SNR and by using a probabilistic independent component analysis (ICA) (Beckmann and Smith, 2004). A preliminary evaluation showed that on average, temporal SNR was 70±15 for the case of no prospective correction, and 67±11 with prospective correction, respectively. Despite the absence of significant differences in the group analysis, substantial variation is seen across participants as shown in Figure 5. This inter-subject variation can be most likely attributed to the limited rigidity of the skin-attached marker and personal differences in skin mobility. This is further supported by applying retrospective correction to the prospectively corrected data. In this case, tSNR increases to 75±9 and is comparable to the tSNR from data with retrospective correction alone, 78±13. To analyse the effect of prospective and retrospective motion correction, the ICA signals derived from the BOLD response were Pearson-correlated with the measured 6DoF motion components, thus providing a measure of the influence of motion on the detected activation signals. As Figure 5b shows, prospective motion correction with the skin-attached marker has increased signal variance for some of the components, this could be more than undone by the retrospective correction, such that a combination of prospective and retrospective corrections resulted in the weakest motion correlations. What is also noteworthy is that two of the motion DoFs (one rotation and one translation) continue to have a strong influence on the BOLD response, even after retrospective correction. These are hypothesised to be two out-of-plane motions, and thus contribute to the aforementioned spin-history effects, for which retrospective correction alone cannot correct for. It is our intention to perform additional experiments with dental attachment of the marker to verify the current interpretation of these preliminary results.

The above examples covered functional MRI based on a 2D EPI protocol with low spatial resolution. For higher spatial resolution, 3D scanning may be desirable, which is not achievable within a single shot. For multi-shot techniques, no pure retrospective correction is available to account for motion-induced data inconsistencies, therefore external real-time correction appears to be especially advantageous. In their recent study, Todd et al. have evaluated the performance of 3D EPI with prospective motion correction based on the same external optical motion tracking system under conditions of no motion, as well as slow and fast motion (Todd et al., 2015). Their results show a consistent increase in tSNR especially in the motion conditions as well as more robust activation detected with prospective correction.

For genuinely small motions and relatively coarse voxel sizes, prospective motion correction has difficulty showing a clear improvement. This is because the effects exclusively attainable by prospective correction (primarily points 3 and 7, and partly point 11 in Table 1) are relatively weak under these conditions. At the same time, tracking noise and more importantly imperfect marker fixation introduce apparent motion of the imaging volume relative to the head, which in extreme cases of very experienced and motivated participants may become comparable with the true head drifts. If the latter is the case, the apparent motion due to erroneous prospective correction, and other potentially harmful effects such increased variance of ghost suppression efficiency, may decrease temporal SNR and consequently BOLD activations. On the other hand, for more pronounced subject motion

and higher spatial resolution, as was the case in the studies cited in the first half of this section, the benefits of prospective correction prevail.

Beyond motion correction

A number of studies cited above have shown the importance of incorporating the dynamic distortion correction into prospectively-corrected EPI. Although we did not perform similar studies in our lab, in our experience motion is the most relevant cause of dynamic B0 alterations. We therefore expect further improvements if other B0-associated signal alteration pathways are taken into account in future, in particular contrast and dephasing changes upon B0 variations. We hypothesise real-time shim updating to be as important for EPI as prospective motion correction in regaining the original signal quality. Even though field map changes upon small head rotations remain relatively smooth (see Figure 1, 2nd column) necessity of adjusting higher-order shimming settings is apparent if these changes are to be corrected prospectively. Higher-order real-time shim updating, however, remains challenging because of the absence of both reliable detection mechanisms and limited hardware availability capable of the desired dynamic field alterations and is a topic of current research.

Benefits of the accurate motion tracking in the magnet bore extend far beyond prospective motion correction. One possible relevant example is the correction of simultaneous electroencephalography (EEG) and fMRI. Independent accurate and high-temporal resolution motion readings allow one to decouple interaction between the gradient-induced voltages in EEG electrodes and ballistocardiographic head motions, resulting in an EEG quality previously unattainable in the magnetic field in presence of EPI-related gradient activity (Körbl et al., 2016; LeVan et al., 2016, 2013). Maziero et al. have further demonstrated a combination of prospectively-corrected EPI-fMRI with simultaneous EEG recordings (Maziero et al., 2016).

Conclusions

Due to the low sensitivity of the BOLD-fMRI, long scanning is typically required. Temporal fluctuations in the MR signal arising due to motion reduce statistical significance of the activation maps and increase the likelihood of false activations. Motion correction is therefore an essential tool for a successful fMRI data analysis. Retrospective motion correction techniques are now commonplace and are incorporated into a wide range of fMRI analysis toolboxes. These techniques are advantageous due to robustness, sequence independence and minimal impact on the fMRI study setup. Retrospective techniques however, do not provide an intra-volume correction, nor can these techniques correct for the spin-history effects. The application of prospective motion correction in fMRI however appears to be effective in reducing false positives and increasing sensitivity when compared to retrospective techniques, particularly in the cases of substantial motion. Especially advantageous in this regard is the combination of prospective motion correction with dynamic distortion correction. Nevertheless, none of the recent methods are able to entirely recover activations in presence of motion that would be comparable to no-motion conditions. This is most likely due to the B0 induced distortion and contrast variations and may be

attained in the future by real-time shim updating or advanced model-based image reconstruction. The evidence of the usability of prospective motion correction for resting-state fMRI is limited at present, but it is reasonable to assume a similar pattern, expecting prospective correction to be more effective in subject groups affected by motion or for studies requiring high spatial resolution.

Acknowledgments

Grant support:

NIH grant numbers 2R01 DA021146

References

Alhamud A, Tisdall MD, Hess AT, Hasan KM, Meintjes EM, van der Kouwe AJW. Volumetric navigators for real-time motion correction in diffusion tensor imaging. Magn. Reson. Med. 2012; 68:1097–1108. [PubMed: 22246720]

Atkinson D, Hill DLG. Reconstruction after rotational motion. Magn. Reson. Med. 2003; 49:183–187. [PubMed: 12509836]

Barth M, Breuer F, Koopmans PJ, Norris DG, Poser BA. Simultaneous multislice (SMS) imaging techniques. Magn. Reson. Med. 2016; 75:63–81. [PubMed: 26308571]

Beall EB, Lowe MJ. SimPACE: generating simulated motion corrupted BOLD data with synthetic-navigated acquisition for the development and evaluation of SLOMOCO: a new, highly effective slicewise motion correction. NeuroImage. 2014; 101:21–34. [PubMed: 24969568]

Beckmann CF, Smith SM. Probabilistic independent component analysis for functional magnetic resonance imaging. IEEE Trans. Med. Imaging. 2004; 23:137–152. [PubMed: 14964560]

Bettinardi V, Scardaoni R, Gilardi MC, Rizzo G, Perani D, Paulesu E, Striano G, Triulzi F, Fazio F. Head holder for PET, CT, and MR studies. J. Comput. Assist. Tomogr. 1991; 15:886–892. [PubMed: 1885820]

Bhagalia R, Kim B. Spin saturation artifact correction using slice-to-volume registration motion estimates for fMRI time series. Med. Phys. 2008; 35:424–434. [PubMed: 18383662]

Boegle R, Maclaren J, Zaitsev M. Combining prospective motion correction and distortion correction for EPI: towards a comprehensive correction of motion and susceptibility-induced artifacts. Magn. Reson. Mater. Phys. Biol. Med. 2010; 23:263–273.

Carp J. Optimizing the order of operations for movement scrubbing: Comment on Power et al. NeuroImage. 2013; 76:436–438. [PubMed: 22227884]

Chen N, Wyrwicz AM. Removal of EPI Nyquist ghost artifacts with two-dimensional phase correction. Magn. Reson. Med. 2004; 51:1247–1253. [PubMed: 15170846]

Cox RW. AFNI: software for analysis and visualization of functional magnetic resonance neuroimages. Comput. Biomed. Res. Int. J. 1996; 29:162–173.

de Bie HMA, Boersma M, Wattjes MP, Adriaanse S, Vermeulen RJ, Oostrom KJ, Huisman J, Veltman DJ, Delemarre-Van de Waal HA. Preparing children with a mock scanner training protocol results in high quality structural and functional MRI scans. Eur. J. Pediatr. 2010; 169:1079–1085. [PubMed: 20225122]

Deichmann R, Josephs O, Hutton C, Corfield DR, Turner R. Compensation of susceptibility-induced BOLD sensitivity losses in echo-planar fMRI imaging. NeuroImage. 2002; 15:120–135. [PubMed: 11771980]

Derbyshire JA, Wright GA, Henkelman RM, Hinks RS. Dynamic scan-plane tracking using MR position monitoring. J. Magn. Reson. Imaging. 1998; 8:924–932. [PubMed: 9702895]

Dymerska B, Poser BA, Bogner W, Visser E, Eckstein K, Cardoso P, Barth M, Trattnig S, Robinson SD. Correcting dynamic distortions in 7T echo planar imaging using a jittered echo time sequence. Magn. Reson. Med. 2015

Eviatar, H., Saunders, JK., Hoult, DI. Motion compensation by gradient adjustment. Presented at the Proceedings of the International Society for Magnetic Resonance n Medicine; Vancouver. 1997. p. 1898

Eviatar, H., Schattka, B., Sharp, JC., Rendell, J., Alexander, ME. Real time head motion correction for functional MRI. Presented at the Proceedings of the International Society for Magnetic Resonance in Medicine; Philadelphia. 1999. p. 269

Faraji-Dana Z, Tam F, Chen JJ, Graham SJ. A robust method for suppressing motion-induced coil sensitivity variations during prospective correction of head motion in fMRI. Magn. Reson. Imaging. 2016; 34:1206–1219. [PubMed: 27451407]

Feinberg DA, Setsompop K. Ultra-fast MRI of the human brain with simultaneous multi-slice imaging. J. Magn. Reson. 2013; 229:90–100. [PubMed: 23473893]

Field AS, Yen YF, Burdette JH, Elster AD. False cerebral activation on BOLD functional MR images: study of low-amplitude motion weakly correlated to stimulus. AJNR Am. J. Neuroradiol. 2000; 21:1388–1396. [PubMed: 11003269]

Forman C, Aksoy M, Hornegger J, Bammer R. Self-encoded marker for optical prospective head motion correction in MRI. Med. Image Comput. Comput.-Assist. Interv. 2010; 13:259–266. [PubMed: 20879239]

Friston KJ, Ashburner J, Frith CD, Poline J-B, Heather JD, Frackowiak RSJ. Spatial registration and normalization of images. Hum. Brain Mapp. 1995; 3:165–189.

Friston KJ, Williams S, Howard R, Frackowiak RSJ, Turner R. Movement-Related effects in fMRI time-series. Magn. Reson. Med. 1996; 35:346–355. [PubMed: 8699946]

Fu ZW, Wang Y, Grimm RC, Rossman PJ, Felmlee JP, Riederer SJ, Ehman RL. Orbital navigator echoes for motion measurements in magnetic resonance imaging. Magn. Reson. Med. 1995; 34:746–753. [PubMed: 8544696]

Gallichan D, Marques JP, Gruetter R. Retrospective correction of involuntary microscopic head movement using highly accelerated fat image navigators (3D FatNavs) at 7T. Magn. Reson. Med. 2016; 75:1030–1039. [PubMed: 25872755]

Godenschweger F, Kägebein U, Stucht D, Yarach U, Sciarra A, Yakupov R, Lüsebrink F, Schulze P, Speck O. Motion correction in MRI of the brain. Phys. Med. Biol. 2016; 61:R32–R56. [PubMed: 26864183]

Goebel R, Esposito F, Formisano E. Analysis of functional image analysis contest (FIAC) data with brainvoyager QX: From single-subject to cortically aligned group general linear model analysis and self-organizing group independent component analysis. Hum. Brain Mapp. 2006; 27:392–401. [PubMed: 16596654]

Griswold MA, Jakob PM, Heidemann RM, Nittka M, Jellus V, Wang J, Kiefer B, Haase A. Generalized autocalibrating partially parallel acquisitions (GRAPPA). Magn. Reson. Med. 2002; 47:1202–1210. [PubMed: 12111967]

Hajnal JV, Myers R, Oatridge A, Schwieso JE, Young IR, Bydder GM. Artifacts due to stimulus correlated motion in functional imaging of the brain. Magn. Reson. Med. 1994; 31:283–291. [PubMed: 8057799]

Haller S, Bartsch AJ. Pitfalls in FMRI. Eur. Radiol. 2009; 19:2689–2706. [PubMed: 19504107]

Hennel F. Two-dimensional deghosting for EPI. Magn. Reson. Mater. Phys. Biol. Med. 1999; 9:134–137.

Herbst M, Maclaren J, Lovell-Smith C, Sostheim R, Egger K, Harloff A, Korvink J, Hennig J, Zaitsev M. Reproduction of motion artifacts for performance analysis of prospective motion correction in MRI. Magn. Reson. Med. 2014; 71:182–190. [PubMed: 23440737]

Hutton C, Andersson J, Deichmann R, Weiskopf N. Phase informed model for motion and susceptibility. Hum. Brain Mapp. 2013; 34:3086–3100. [PubMed: 22736546]

Hutton C, Josephs O, Stadler J, Featherstone E, Reid A, Speck O, Bernarding J, Weiskopf N. The impact of physiological noise correction on fMRI at 7 T. NeuroImage. 2011; 57:101–112. [PubMed: 21515386]

Jenkinson M, Bannister P, Brady M, Smith S. Improved optimization for the robust and accurate linear registration and motion correction of brain images. Neuroimage. 2002; 17:825–841. [PubMed: 12377157]

Jezzard P. Correction of geometric distortion in fMRI data. NeuroImage. 2012; 62:648–651. [PubMed: 21945795]

Körbl K, Jacobs J, Herbst M, Zaitsev M, Schulze-Bonhage A, Hennig J, LeVan P. Marker-based ballistocardiographic artifact correction improves spike identification in EEG-fMRI of focal epilepsy patients. Clin. Neurophysiol. 2016; 127:2802–2811. [PubMed: 27417056]

Lamberton F, Delcroix N, Grenier D, Mazoyer B, Joliot M. A new EPI-based dynamic field mapping method: application to retrospective geometrical distortion corrections. J. Magn. Reson. Imaging. 2007; 26:747–755. [PubMed: 17729370]

Lauzon ML, Rutt BK. Generalized K-space analysis and correction of motion effects in MR imaging. Magn Reson Med. 1993; 30:438–446. [PubMed: 8255191]

Lee CC, Grimm RC, Manduca A, Felmlee JP, Ehman RL, Riederer SJ, Jack CR. A prospective approach to correct for inter-image head rotation in fMRI. Magn. Reson. Med. 1998; 39:234–243. [PubMed: 9469706]

Lee CC, Jack CR, Grimm RC, Rossman PJ, Felmlee JP, Ehman RL, Riederer SJ. Real-time adaptive motion correction in functional MRI. Magn. Reson. Med. 1996; 36:436–444. [PubMed: 8875415]

Lemmin T, Ganesh G, Gassert R, Burdet E, Kawato M, Haruno M. Model-based attenuation of movement artifacts in fMRI. J. Neurosci. Methods. 2010; 192:58–69. [PubMed: 20654648]

LeVan P, Maclaren J, Herbst M, Sostheim R, Zaitsev M, Hennig J. Ballistocardiographic artifact removal from simultaneous EEG-fMRI using an optical motion-tracking system. NeuroImage. 2013; 75:1–11. [PubMed: 23466939]

LeVan P, Zhang S, Knowles B, Zaitsev M, Hennig J. EEG-fMRI Gradient Artifact Correction by Multiple Motion-Related Templates. IEEE Trans. Biomed. Eng. 2016

Lu Z, Phua KS, Huang W, Hong X, Nasrallah FA, Chuang K-H, Guan C. Combining EPI and motion correction for fMRI human brain images with big motion. Annu. Int. Conf. IEEE Eng. Med. Biol. Soc. 2015; 2015:5449–5452.

Lueken U, Muehlhan M, Evens R, Wittchen H-U, Kirschbaum C. Within and between session changes in subjective and neuroendocrine stress parameters during magnetic resonance imaging: A controlled scanner training study. Psychoneuroendocrinology. 2012; 37:1299–1308. [PubMed: 22309826]

Lund TE, Nørgaard MD, Rostrup E, Rowe JB, Paulson OB. Motion or activity: their role in intra- and inter-subject variation in fMRI. NeuroImage. 2005; 26:960–964. [PubMed: 15955506]

Maclaren J, Armstrong BSR, Barrows RT, Danishad KA, Ernst T, Foster CL, Gumus K, Herbst M, Kadashevich IY, Kusik TP, Li Q, Lovell-Smith C, Prieto T, Schulze P, Speck O, Stucht D, Zaitsev M. Measurement and correction of microscopic head motion during magnetic resonance imaging of the brain. PloS One. 2012; 7:e48088. [PubMed: 23144848]

Maclaren J, Herbst M, Speck O, Zaitsev M. Prospective motion correction in brain imaging: a review. Magn. Reson. Med. 2013; 69:621–636. [PubMed: 22570274]

Maclaren J, Speck O, Stucht D, Schulze P, Hennig J, Zaitsev M. Navigator accuracy requirements for prospective motion correction. Magn. Reson. Med. 2010; 63:162–170. [PubMed: 19918892]

Malisza KL, Buss JL, Bolster RB, de Gervai PD, Woods-Frohlich L, Summers R, Clancy CA, Chudley AE, Longstaffe S. Comparison of spatial working memory in children with prenatal alcohol exposure and those diagnosed with ADHD; A functional magnetic resonance imaging study. J. Neurodev. Disord. 2012; 4:12. [PubMed: 22958510]

Malviya S, Voepel-Lewis T, Eldevik OP, Rockwell DT, Wong JH, Tait AR. Sedation and general anaesthesia in children undergoing MRI and CT: adverse events and outcomes. Br. J. Anaesth. 2000; 84:743–748. [PubMed: 10895749]

Mayer AR, Franco AR, Ling J, Cañive JM. Assessment and quantification of head motion in neuropsychiatric functional imaging research as applied to schizophrenia. J. Int. Neuropsychol. Soc. 2007; 13:839–845. [PubMed: 17697415]

Maziero D, Velasco TR, Hunt N, Payne E, Lemieux L, Salmon CEG, Carmichael DW. Towards motion insensitive EEG-fMRI: Correcting motion-induced voltages and gradient artefact instability in EEG using an fMRI prospective motion correction (PMC) system. NeuroImage. 2016; 138:13–27. [PubMed: 27157789]

Menon V, Lim KO, Anderson JH, Johnson J, Pfefferbaum A. Design and efficacy of a head-coil bite bar for reducing movement-related artifacts during functional MRI scanning. Behav. Res. Methods Instrum. Comput. 1997; 29:589–594.

Muraskin J, Ooi MB, Goldman RI, Krueger S, Thomas WJ, Sajda P, Brown TR. Prospective active marker motion correction improves statistical power in BOLD fMRI. NeuroImage. 2013; 68:154–161. [PubMed: 23220430]

Muresan L, Renken R, Roerdink JBTM, Duifhuis H. Automated correction of spin-history related motion artefacts in fMRI: simulated and phantom data. IEEE Trans. Biomed. Eng. 2005; 52:1450–1460. [PubMed: 16119241]

Murphy K, Birn RM, Bandettini PA. Resting-state fMRI confounds and cleanup. NeuroImage. 2013; 80:349–359. [PubMed: 23571418]

Nehrke K, Börnert P. Prospective correction of affine motion for arbitrary MR sequences on a clinical scanner. Magn. Reson. Med. 2005; 54:1130–1138. [PubMed: 16200564]

Oakes TR, Johnstone T, Ores Walsh KS, Greischar LL, Alexander AL, Fox AS, Davidson RJ. Comparison of fMRI motion correction software tools. NeuroImage. 2005; 28:529–543. [PubMed: 16099178]

Ooi MB, Aksoy M, Maclaren J, Watkins RD, Bammer R. Prospective motion correction using inductively coupled wireless RF coils. Magn. Reson. Med. 2013a; 70:639–647. [PubMed: 23813444]

Ooi MB, Krueger S, Muraskin J, Thomas WJ, Brown TR. Echo-planar imaging with prospective slice-by-slice motion correction using active markers. Magn. Reson. Med. 2011; 66:73–81. [PubMed: 21695720]

Ooi MB, Muraskin J, Zou X, Thomas WJ, Krueger S, Aksoy M, Bammer R, Brown TR. Combined prospective and retrospective correction to reduce motion-induced image misalignment and geometric distortions in EPI. Magn. Reson. Med. 2013b; 69:803–811. [PubMed: 22499027]

Power JD, Mitra A, Laumann TO, Snyder AZ, Schlaggar BL, Petersen SE. Methods to detect, characterize, and remove motion artifact in resting state fMRI. NeuroImage. 2014; 84:320–341. [PubMed: 23994314]

Pruessmann KP, Weiger M, Scheidegger MB, Boesiger P. SENSE: sensitivity encoding for fast MRI. Magn. Reson. Med. 1999; 42:952–962. [PubMed: 10542355]

Roemer PB, Edelstein WA, Hayes CE, Souza SP, Mueller OM. The NMR phased array. Magn. Reson. Med. 1990; 16:192–225. [PubMed: 2266841]

Rotenberg D, Chiew M, Ranieri S, Tam F, Chopra R, Graham SJ. Real-time correction by optical tracking with integrated geometric distortion correction for reducing motion artifacts in functional MRI. Magn. Reson. Med. 2013; 69:734–748. [PubMed: 22585554]

Schulz J, Siegert T, Bazin P-L, Maclaren J, Herbst M, Zaitsev M, Turner R. Prospective slice-by-slice motion correction reduces false positive activations in fMRI with task-correlated motion. NeuroImage. 2014; 84:124–132. [PubMed: 23954484]

Schulz J, Siegert T, Reimer E, Labadie C, Maclaren J, Herbst M, Zaitsev M, Turner R. An embedded optical tracking system for motion-corrected magnetic resonance imaging at 7T. Magn. Reson. Mater. Phys. Biol. Med. 2012; 25:443–453.

Sengupta S, Tadanki S, Gore JC, Welch EB. Prospective real-time head motion correction using inductively coupled wireless NMR probes. Magn. Reson. Med. 2014; 72:971–985. [PubMed: 24243810]

Seto E, Sela G, McIlroy WE, Black SE, Staines WR, Bronskill MJ, McIntosh AR, Graham SJ. Quantifying head motion associated with motor tasks used in fMRI. NeuroImage. 2001; 14:284–297. [PubMed: 11467903]

Sostheim, R., Maclaren, J., Testud, F., Zaitsev, M. Predicting Field Distortions in the Human Brain Using a Susceptibility Model of the Head. Presented at the Proceedings of the International Society for Magnetic Resonance in Medicine; Melbourne. 2012. p. 3386

Speck O, Hennig J, Zaitsev M. Prospective real-time slice-by-slice motion correction for fMRI in freely moving subjects. Magn. Reson. Mater. Phys. Biol. Med. 2006; 19:55–61.

Speck, O., Zaitsev, M. Real-Time Prospective Slice-By-Slice Motion Correction for fMRI in Freely Moving Subjects. Presented at the Proceedings of the International Society for Magnetic Resonance in Medicine; Seattle. 2006. p. 241

Stucht D, Danishad KA, Schulze P, Godenschweger F, Zaitsev M, Speck O. Highest Resolution In Vivo Human Brain MRI Using Prospective Motion Correction. PloS One. 2015; 10:e0133921. [PubMed: 26226146]

Thesen S, Heid O, Mueller E, Schad LR. Prospective acquisition correction for head motion with image-based tracking for real-time fMRI. Magn. Reson. Med. 2000; 44:457–465. [PubMed: 10975899]

Tian, Q., Gong, E., Leuze, C., W, U., Pauli, J., McNab, J. Effects of motion on coupling of coil elements and parallel imaging reconstruction at 3T and 7T. Presented at the Proceedings of International Society for Magnetic Resonance in Medicine; Toronto. 2015. p. 2419

Todd N, Josephs O, Callaghan MF, Lutti A, Weiskopf N. Prospective motion correction of 3D echo-planar imaging data for functional MRI using optical tracking. NeuroImage. 2015; 113:1–12. [PubMed: 25783205]

Tsao J. Ultrafast imaging: Principles, pitfalls, solutions, and applications. J. Magn. Reson. Imaging. 2010; 32:252–266. [PubMed: 20677249]

Van de Walle R, Lemahieu I, Achten E. Magnetic resonance imaging and the reduction of motion artifacts: review of the principles. Technol Health Care. 1997; 5:419–435. [PubMed: 9696161]

van der Kouwe AJW, Benner T, Dale AM. Real-time rigid body motion correction and shimming using cloverleaf navigators. Magn. Reson. Med. 2006; 56:1019–1032. [PubMed: 17029223]

Van Dijk KRA, Sabuncu MR, Buckner RL. The influence of head motion on intrinsic functional connectivity MRI. NeuroImage. 2012; 59:431–438. [PubMed: 21810475]

Vannesjo SJ, Graedel NN, Kasper L, Gross S, Busch J, Haeberlin M, Barmet C, Pruessmann KP. Image reconstruction using a gradient impulse response model for trajectory prediction. Magn. Reson. Med. 2016; 76:45–58. [PubMed: 26211410]

Ward HA, Riederer SJ, Grimm RC, Ehman RL, Felmlee JP, Jack CR. Prospective multiaxial motion correction for fMRI. Magn. Reson. Med. 2000; 43:459–469. [PubMed: 10725890]

Welch EB, Manduca A, Grimm RC, Ward HA, Jack CR. Spherical navigator echoes for full 3D rigid body motion measurement in MRI. Magn. Reson. Med. 2002; 47:32–41. [PubMed: 11754440]

White N, Roddey C, Shankaranarayanan A, Han E, Rettmann D, Santos J, Kuperman J, Dale A. PROMO: Real-time prospective motion correction in MRI using image-based tracking. Magn. Reson. Med. 2010; 63:91–105. [PubMed: 20027635]

Windram J, Grosse-Wortmann L, Shariat M, Greer M-L, Crawford MW, Yoo S-J. Cardiovascular MRI without sedation or general anesthesia using a feed-and-sleep technique in neonates and infants. Pediatr. Radiol. 2012; 42:183–187. [PubMed: 21861089]

Wood ML, Henkelman RM. MR image artifacts from periodic motion. Med. Phys. 1985; 12:143. [PubMed: 4000069]

Wu DH, Lewin JS, Duerk JL. Inadequacy of motion correction algorithms in functional MRI: role of susceptibility-induced artifacts. J. Magn. Reson. Imaging. 1997; 7:365–370. [PubMed: 9090592]

Xiang Q-S, Ye FQ. Correction for geometric distortion and N/2 ghosting in EPI by phase labeling for additional coordinate encoding (PLACE). Magn. Reson. Med. 2007; 57:731–741. [PubMed: 17390358]

Yan C-G, Cheung B, Kelly C, Colcombe S, Craddock RC, Di Martino A, Li Q, Zuo X-N, Castellanos FX, Milham MP. A comprehensive assessment of regional variation in the impact of head micromovements on functional connectomics. NeuroImage. 2013; 76:183–201. [PubMed: 23499792]

Yancey SE, Rotenberg DJ, Tam F, Chiew M, Ranieri S, Biswas L, Anderson KJT, Baker SN, Wright GA, Graham SJ. Spin-history artifact during functional MRI: potential for adaptive correction. Med. Phys. 2011; 38:4634–4646. [PubMed: 21928636]

Yang S, Ross TJ, Zhang Y, Stein EA, Yang Y. Head motion suppression using real-time feedback of motion information and its effects on task performance in fMRI. NeuroImage. 2005; 27:153–162. [PubMed: 16023040]

Yarach U, Luengviriya C, Danishad A, Stucht D, Godenschweger F, Schulze P, Speck O. Correction of gradient nonlinearity artifacts in prospective motion correction for 7T MRI. Magn. Reson. Med. 2015; 73:1562–1569. [PubMed: 24798889]

Yarach U, Luengviriya C, Stucht D, Godenschweger F, Schulze P, Speck O. Correction of B 0-induced geometric distortion variations in prospective motion correction for 7T MRI. Magn. Reson. Mater. Phys. Biol. Med. 2016; 29:319–332.

Yeo DTB, Fessler JA, Kim B. Concurrent correction of geometric distortion and motion using the map-slice-to-volume method in echo-planar imaging. Magn. Reson. Imaging. 2008; 26:703–714. [PubMed: 18280077]

Yuan W, Altaye M, Ret J, Schmithorst V, Byars AW, Plante E, Holland SK. Quantification of head motion in children during various fMRI language tasks. Hum. Brain Mapp. 2009; 30:1481–1489. [PubMed: 18636549]

Zahneisen B, Ernst T. Homogeneous coordinates in motion correction. Magn. Reson. Med. 2016; 75:274–279. [PubMed: 25648318]

Zahneisen B, Keating B, Ernst T. Propagation of Calibration Errors in Prospective Motion Correction Using External Tracking. Magn. Reson. Med. 2014a; 72:381–388. [PubMed: 24123287]

Zahneisen B, Keating B, Singh A, Herbst M, Ernst T. Reverse retrospective motion correction. Magn. Reson. Med. 2016; 75:2341–2349. [PubMed: 26140504]

Zahneisen B, Lovell-Smith C, Herbst M, Zaitsev M, Speck O, Armstrong B, Ernst T. Fast noniterative calibration of an external motion tracking device. Magn. Reson. Med. 2014b; 71:1489–1500. [PubMed: 23788117]

Zaitsev, M., Dold, C., Hennig, J., Speck, O. Prospective Real-Time Slice-by-Slice 3D Motion Correction for EPI Using an External Optical Motion Tracking System. Presented at the Proceedings of the International Society for Magnetic Resonance in Medicine; Kyoto. 2004. p. 517

Zaitsev M, Dold C, Sakas G, Hennig J, Speck O. Magnetic resonance imaging of freely moving objects: prospective real-time motion correction using an external optical motion tracking system. NeuroImage. 2006; 31:1038–1050. [PubMed: 16600642]

Zaitsev M, Maclaren J, Herbst M. Motion artifacts in MRI: A complex problem with many partial solutions. J. Magn. Reson. Imaging. 2015; 42:887–901. [PubMed: 25630632]

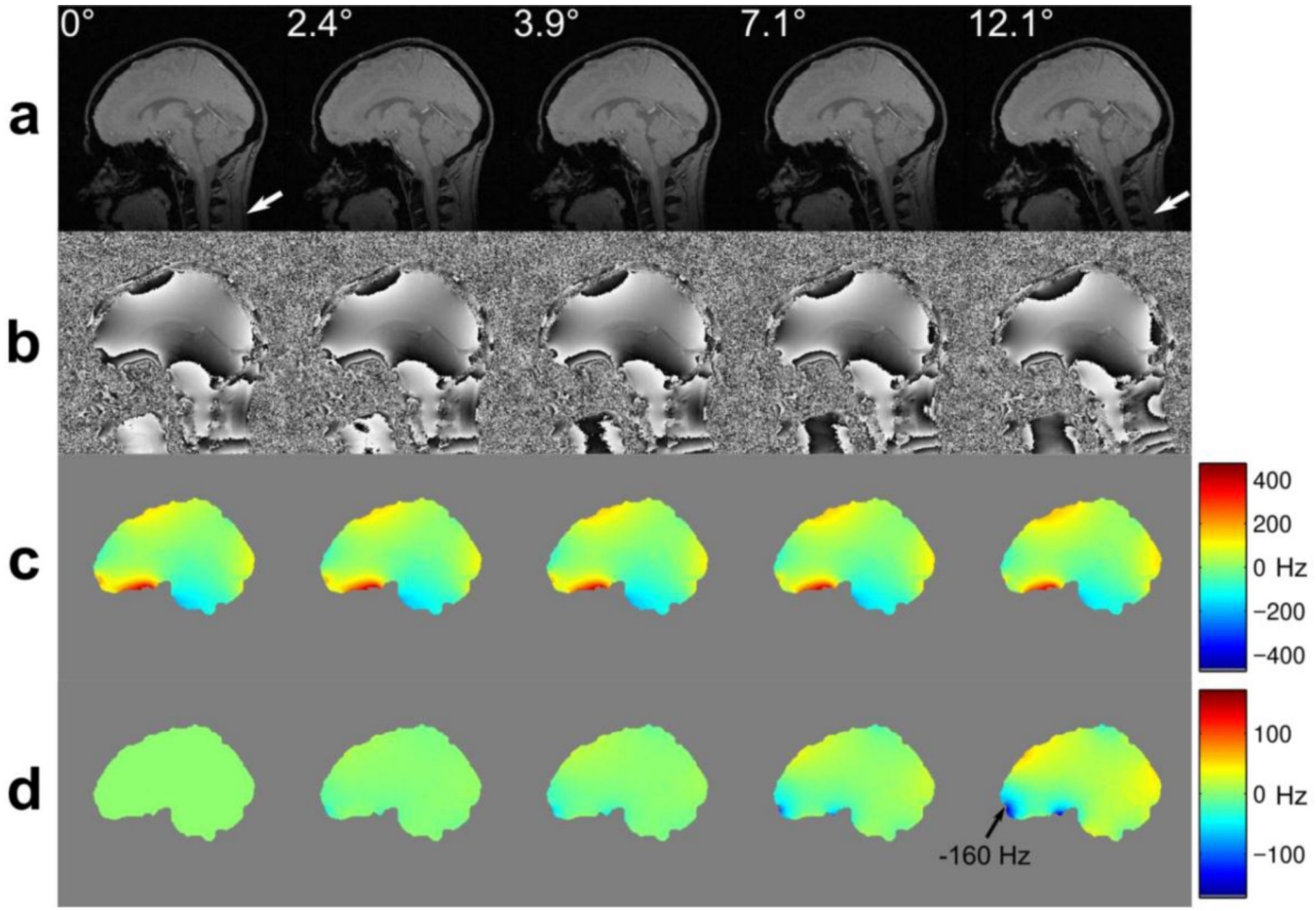

Figure 1.

A demonstration of magnetic susceptibility effects on the B0 field distortions in the human brain during motion. In this example, acquired at 3T the subject rotated his head backwards in four steps. Prospective motion correction was applied while imaging with a modified field mapping sequence: (a) gradient echo magnitude images showing that the brain and skull remain aligned, due to prospective motion correction, while the neck deforms slightly, due to non-rigid effects (see white arrows); (b) the corresponding field maps, obtained directly from the scanner; (c) field maps after masking and unwrapping; (d) difference images between each field map in (c) and the field map obtained in the 0° reference position. Image data were presented in (Maclaren et al., 2013).

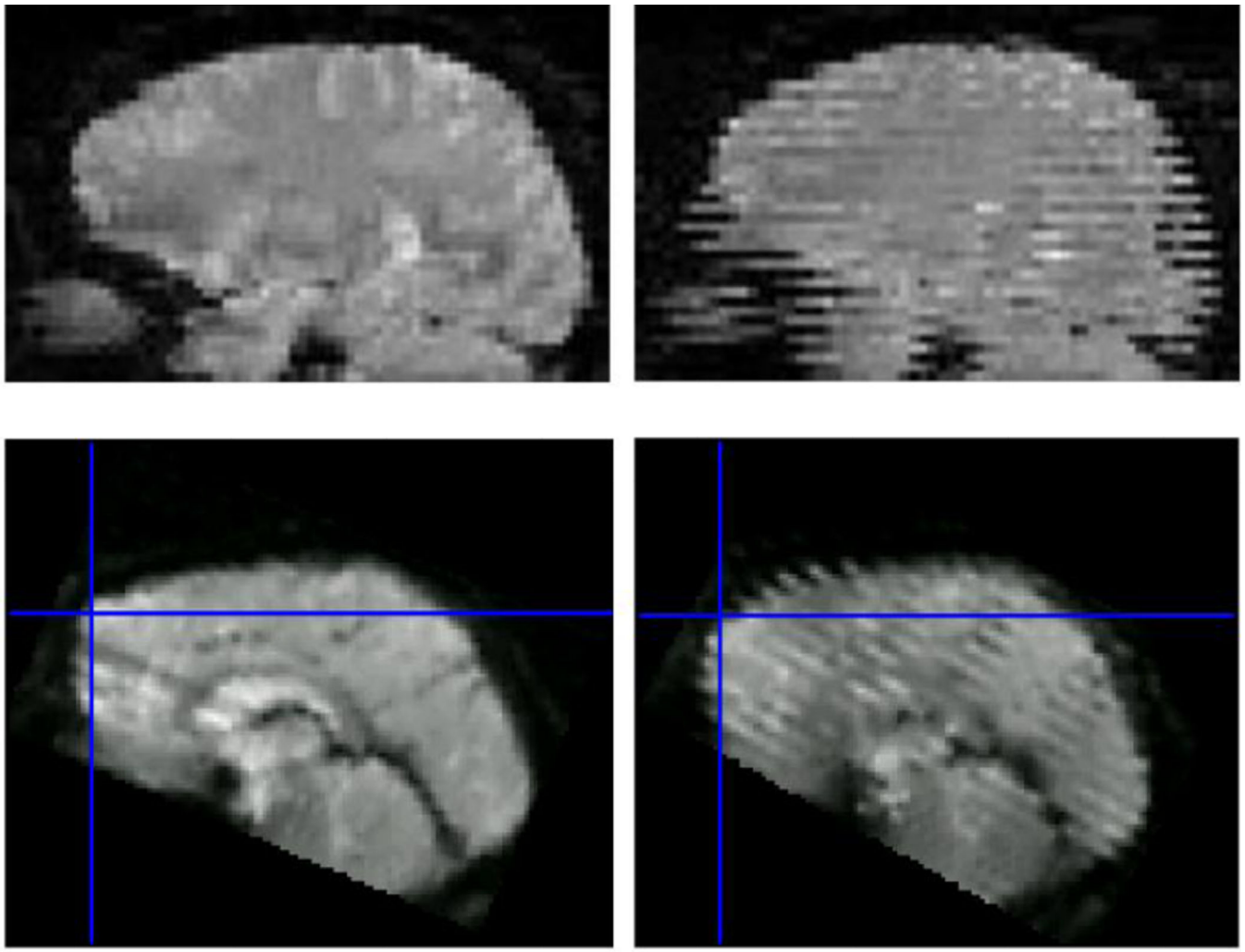

Figure 2.

volume distortions and spin history effects, sagittal reformations of axially acquired data. Top row, left: volume free of distortions and spin-history effects; top-right: volume acquired in presence of left-right rotation and without prospective motion correction. Interleaved slice ordering is obvious due to the misalignment between the odd and even interleaves. Bottom row, left: volume acquired with sequential slice ordering in a presence of a single abrupt nodding motion; bottom-right: similar motion but interleaved acquisition. Top row is from (Speck et al., 2006); Bottom row from http://imaging.mrc-cbu.cam.ac.uk/imaging/CommonArtefacts.

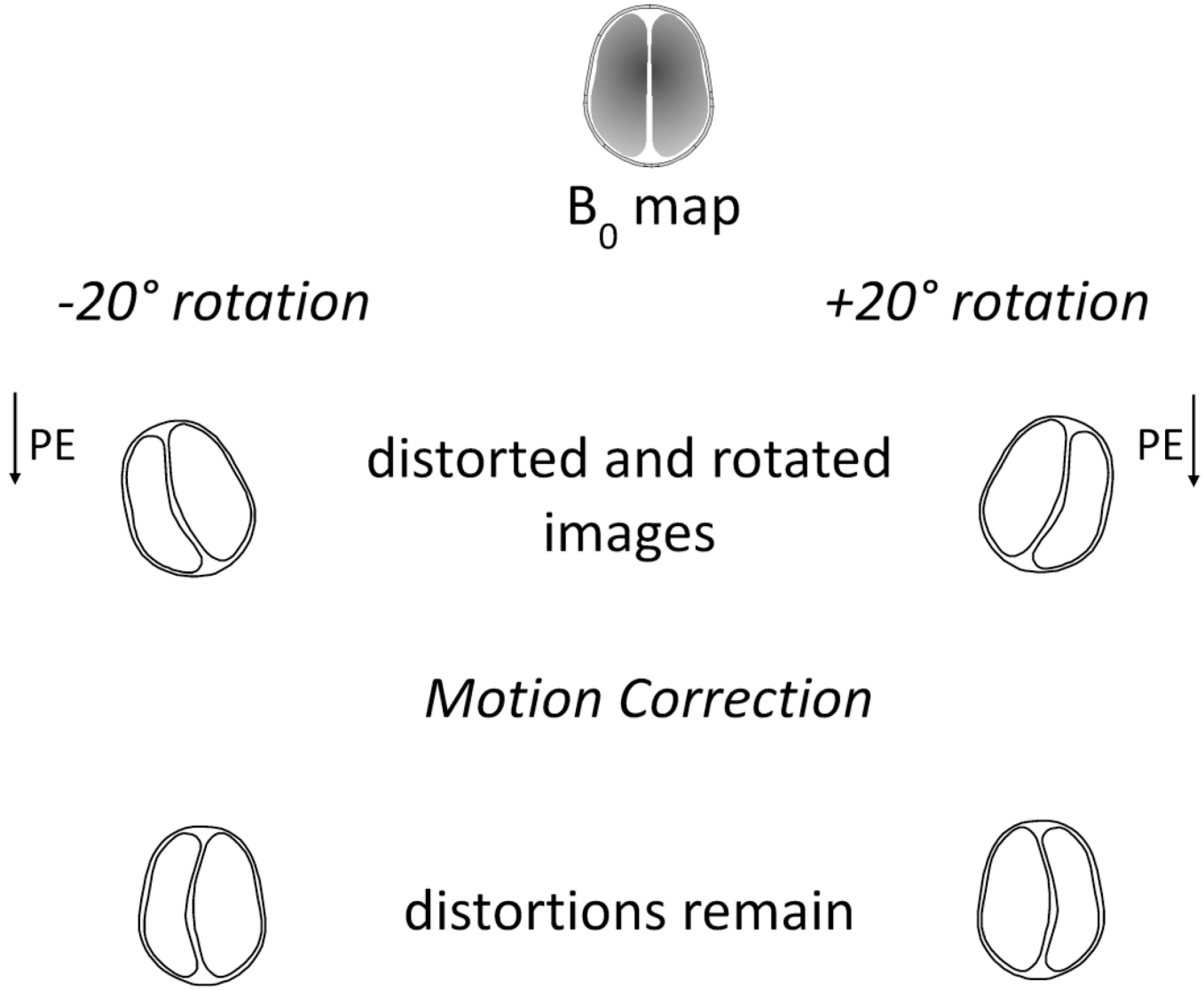

Figure 3.
Cartoon demonstrating the interference between distortions and motion in EPI in the case of retrospective motion correction. Geometric distortions in EPI is a process consisting of one-dimensional pixel shifts along the phase-encoding direction. If motion correction precedes distortion correction, as shown above, the resultant distortions will involve two spatial dimensions and are harder to account for.

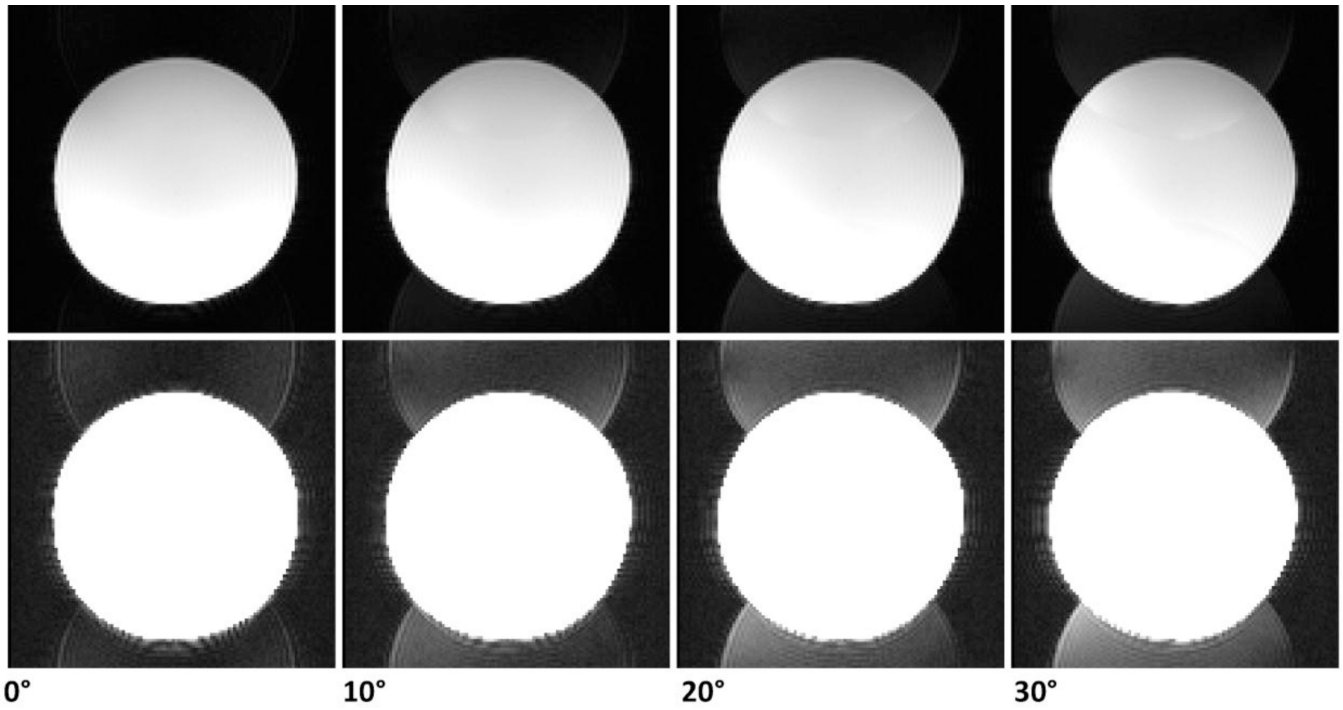

Figure 4.

Phantom images acquired with different in-plane rotation angles. Image intensity within each row is the same between the images to enable comparisons. The top raw was windowed optimally, whereas the bottom raw shows the same images overscaled to make the N/2 ghost clearly visible to the naked eye. The insufficiency of the vendor-provided N/2 ghost correction is apparent even for in-plane rotations of 10°. Imaging parameters: EPI, no parallel acceleration, matrix size 112×112, FOV 224 mm, slice thickness 2mm, echo time 34ms, 7/8 partial Fourier acquisition.

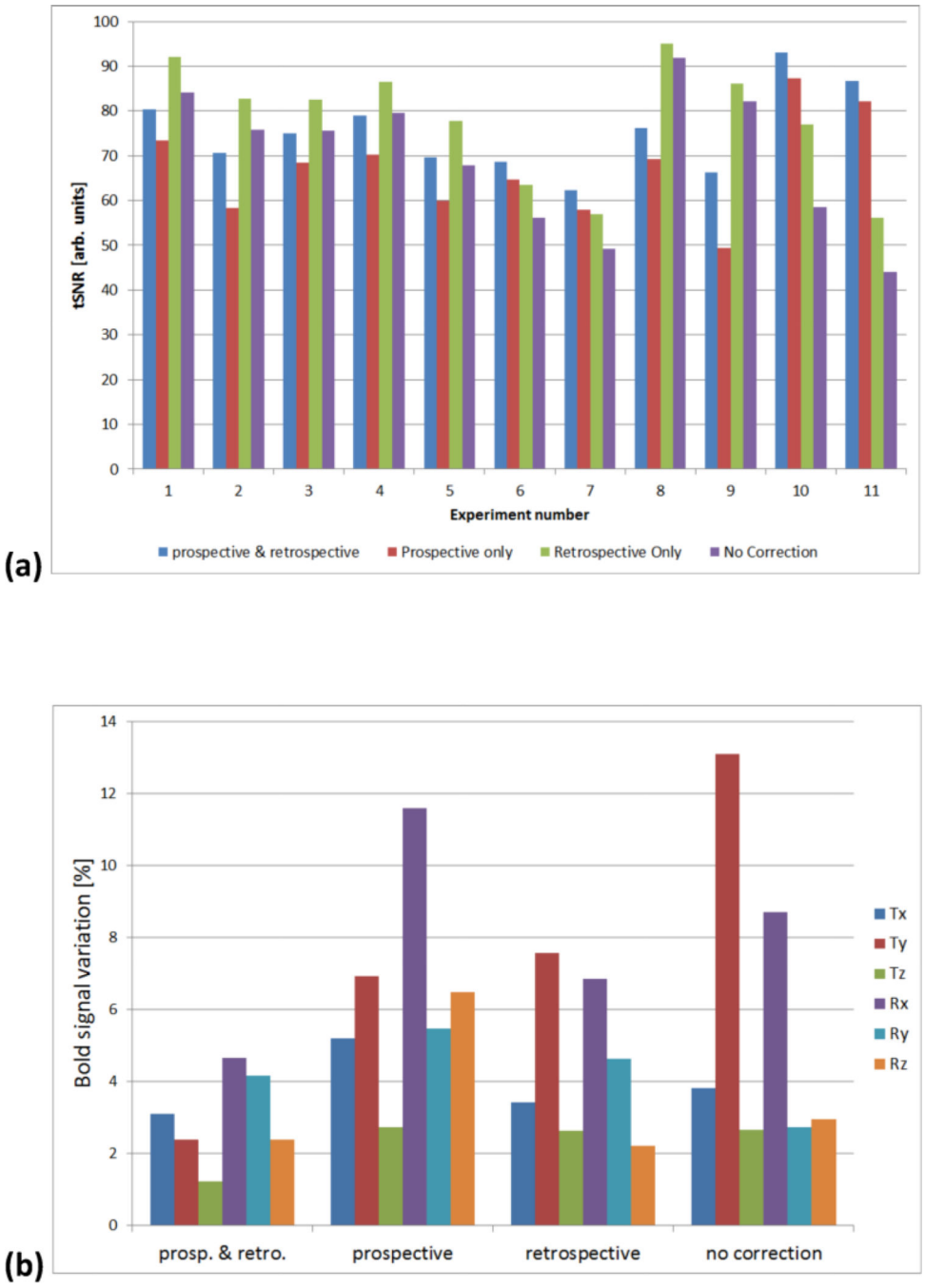

Figure 5.

(a) Graph showing tSNR results for each subject from fMRI data with various motion correction states. A large variation in the effect of prospective motion correction can be observed. Pure prospective correction shows a general tendency to lower tSNR, however upon a combination with retrospective correction improvements can be observed in some subjects. Marker fixation to the skin is theorised to be the cause of these variations. (b) Group analysis showing the contribution of each motion DoF to the BOLD signal using different motion correction techniques. ICA analysis produced signals corresponding to a

fraction of the overall BOLD signal variance. Signal variance was then attributed to motion if a correlation was detected to one of the 6 measured motion DoF.

Table 1

Effects of head motion on fMRI data grouped by a physical source or scanner subsystem. Severity of the effect is ranked from low to high, where low implies little or no effect on the fMRI data, and high implies considerable data corruption leading to an erroneous data analysis.

source		effect	consequence	severity
RF transmit	1.	motion of the object under investigation relative to the stationary, generally inhomogeneous transmit radiofrequency (TX-RF) fields	contrast modulation	low *
	2.	alteration of the TX-RF field(s) due to the coil loading changes and wave phenomena	contrast modulation	low *
RF receive	3.	motion of the object with respect to the signal preparation or slice/slab RF excitation pulses	contrast modulation	high
	4.	motion of the object relative to the stationary receiver coils and the corresponding radiofrequency fields (RX-RF), i.e. receiver coil sensitivities	intensity modulation	high
	5.	alteration of the spatial distribution of the RX-RF fields due to the coil loading changes, wave phenomena or motion of the coils in case of the flexible coils	intensity modulation	medium *
spatial encoding	6.	motion of the object, including internal structures relative to the image encoding coordinates defined by the gradient pulses, receiver frequency and phase offsets	partial-volume effect modulation	high
	7.	motion of the object during the acquisition of multi-slice packages	inconsistent 3D data	medium
	8.	local variations in spatial resolution corresponding to different positions due to the non-linearity of the spatial encoding fields	modulation of distortions or blurring	low †
Shimming & susceptibility	9.	motion of the object-generated magnetic field inhomogeneities relative to the stationary B0 inhomogeneities and the stationary shim coils.	B0 modulation	medium
	10.	alteration of the susceptibility-induced field distributions associated with a rotation of the object with respect to the B0 direction	B0 modulation	medium *
local B0 modulation	11.	alteration of the effective spatial encoding due to the changes in the local field inhomogeneities (motion to distortion interaction)	modulation of distortions or blurring	medium *
	12.	alterations due to local intra-voxel dephasing	intensity modulation	medium *

The consequence severity is based on the authors' own experiences at 3T and may vary for different protocols and field strengths. In particular, severity tends to increase with higher main field strength for cells marked with asterisk (*), and also increases when a local head-only gradient coil is used for cells marked with dagger (†).